ISSN 1674-1056
http://cpb.iphy.ac.cn
http://iopscience.iop.org/cpb
中国物理 B
Chinese Physics
中国物理
Chinese Physics B

Upstream ion wave excitation in an ion-beam-plasma system

Kai-yang Yi(弋开阳), Jin-Xiu Ma(马锦秀), Zi-an Wei(卫子安), Zheng-yuan Li(李政元)
Citation: Chin. Phys. B . 2018, 27(5): 055201. **doi:** 10.1088/1674-1056/27/5/055201

Journal homepage: http://cpb.iphy.ac.cn; http://iopscience.iop.org/cpb

What follows is a list of articles you may be interested in

Schamel equation in an inhomogeneous magnetized sheared flow plasma with *q*-nonextensive trapped electrons

Shaukat Ali Shan, Qamar-ul-Haque
Chin. Phys. B . 2018, 27(2): 025203. **doi:** 10.1088/1674-1056/27/2/025203

Plural interactions of space charge wave harmonics during the development of two-stream instability

Victor Kulish, Alexander Lysenko, Michael Rombovsky, Vitaliy Koval, Iurii Volk
Chin. Phys. B . 2015, 24(9): 095201. **doi:** 10.1088/1674-1056/24/9/095201

Parametric instabilities in single-walled carbon nanotubes

He Cai-Xia, Jian Yue, Qi Xiu-Ying, Xue Ju-Kui
Chin. Phys. B . 2014, 23(2): 025202. **doi:** 10.1088/1674-1056/23/2/025202

Effects of bi-kappa distributed electrons on dust-ion-acoustic shock waves in dusty superthermal plasmas

M. S. Alam, M. M. Masud, A. A. Mamun
Chin. Phys. B . 2013, 22(11): 115202. **doi:** 10.1088/1674-1056/22/11/115202

Kadomtsev–Petviashvili equation for dust ion-acoustic solitons in pair-ion plasmas

Hafeez Ur-Rehman
Chin. Phys. B . 2013, 22(3): 035202. **doi:** 10.1088/1674-1056/22/3/035202

Upstream ion wave excitation in an ion-beam–plasma system*

Kai-Yang Yi(弋开阳), Jin-Xiu Ma(马锦秀)†, Zi-An Wei(卫子安), and Zheng-Yuan Li(李政元)

Department of Modern Physics and Chinese Academy of Sciences Key Laboratory of Geospace Environment, University of Science and Technology of China, Hefei 230026, China

(Received 30 January 2018; published online 26 April 2018)

Plasma normal modes in ion-beam–plasma systems were experimentally investigated previously only for the waves propagating in the downstream (along the beam) direction. In this paper, the ion wave excitation and propagation in the upstream (against the beam) direction in an ion-beam–plasma system were experimentally studied in a double plasma device. The waves were launched by applying a ramp voltage to a negatively biased excitation grid. Two kinds of wave signals were detected, one is a particle signal composed of burst ions and the other is an ion-acoustic signal arising from the background plasma. These signals were identified by the dependence of the signal velocities on the characteristics of the ramp voltage. The velocity of the burst ion signal increases with the decrease of the rise time and the increase of the peak-to-peak amplitude of the applied ramp voltage while that of the ion-acoustic signal is independent of these parameters. By adjusting these parameters such that the burst ion velocity approaches to the ion-acoustic velocity, the wave–particle interaction can be observed.

Keywords: ion-beam–plasma system, upstream direction, ion-acoustic wave, burst ion

PACS: 52.35.–g, 52.35.Fp, 52.35.Qz **DOI:** 10.1088/1674-1056/27/5/055201

1. Introduction

Beam–plasma systems exist widely in space and laboratory devices and are known as typical examples of non-equilibrium plasmas. Linear and nonlinear waves and instabilities in such systems have been widely investigated during the past few decades[1–12] and have become of interest recently[13–18] since these investigations are of fundamental importance to plasma and space physics. In an ion-beam–plasma system, it is well known that the normal modes propagating in the downstream direction (i.e., along the beam direction) are the fast and the slow waves and the ion-acoustic wave.[2] These modes have been well studied both theoretically and experimentally.[1–5] It is also known theoretically that there is only one normal mode, i.e., the ion-acoustic wave, in the upstream direction (i.e., propagating against the beam).[5] In a drifting plasma with flow velocity much lower than the ion-acoustic speed, the ion-acoustic waves propagating against the flow were investigated in a few experiments.[19,20] However, in the ion-beam–plasma systems, the experimental studies of the excitation and propagation of ion waves in the upstream direction have not been reported.

Previous experiments on ion-wave excitation were often conducted in Q-machine or double-plasma devices (DPDs), mostly in DPDs. One way to launch the ion waves was to apply an excitation voltage to a grid (called excitation grid),[21–23] and the excited wave signals were detected by a movable electrostatic probe. In experiments, using a pulse (or pulsed train of sinusoidal signal) as the excitation voltage, a kind of pseudowave signal was detected to coexist and be in front of the excited ion-acoustic wave.[24] This signal, whose characteristics are totally different from those of the normal modes, was recognized as a burst-ion signal,[21–25] because it was believed that this signal is from the ions bursting out of the sheath of the excitation grid when the grid voltage is suddenly raised (by the applied pulse), i.e., it is the signal of the burst ions directly collected by the probe rather than that of the collective waves. This pseudowave is important because its velocity can be controlled by the applied excitation voltage and, thus, the wave–particle interaction between the ion-acoustic wave and the burst ions can be studied via observing the evolution of the excited signals.[26,27]

Previous observations of the pseudowaves were only in plasmas without stationary ion beams. In an ion-beam–plasma system, the pseudowave and its coexistence with the normal modes were observed and identified only recently in the downstream of the beam.[28] The co-excitation of the pseudowave and the normal mode in the upstream direction of the beam has not been investigated.

This article reports the excitation of the ion-acoustic wave and the burst-ion signal and their interactions in the upstream direction of the beam in an ion-beam–plasma system. The experimental arrangement is described in Section 2. The characteristics of the excited wave signals are presented in Section 3. The signals are identified in Sections 4 and 5 and their interactions are presented in Section 6. Section 7 is a summary of the results.

*Project supported by the National Natural Science Foundation of China (Grant Nos. 11575183 and 11705201).

†Corresponding author. E-mail: jxma@ustc.edu.cn

© 2018 Chinese Physical Society and IOP Publishing Ltd

2. Experiment setup and plasma parameters

The experiment was conducted in a double-plasma device as schematically shown in Fig. 1. The device is divided into two chambers, separated by two separation grids (SG1 and SG2, 60% transparency and 10 mm gap), with multiple dipole magnets surrounding the outer surface. The plasma was generated in the source chamber by the discharge between a cylindrical anode mesh (AM) and a hot cathode consisting of a set of 12 hot filaments (HF) distributed cylindrically, and diffused into the experimental (target) chamber. By applying a negative bias voltage on SG2, a directed ion beam could be produced in the target chamber. The base pressure was $p = 4 \times 10^{-4}$ Pa, and the Ar gas working pressure was $p = 2.0 \times 10^{-2}$ Pa. The discharge voltage and current between the anode and the cathode were 50 V and 0.9 A, respectively.

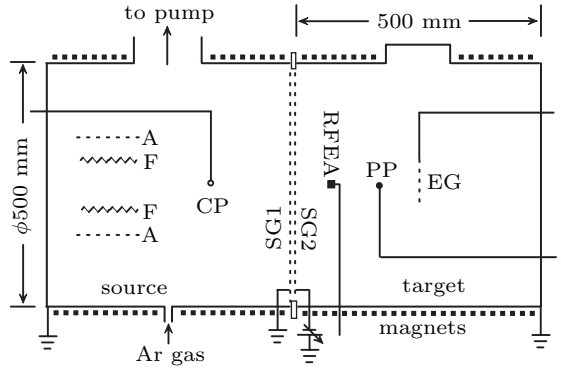


Fig. 1. Schematic diagram of the experimental setup. A: anode, F: filaments, SG: separation grid, CP: cylindrical probe, PP: planar probe, EG: excitation grid, RFEA: retarding field energy analyzer.

Two movable Langmuir probes, a cylindrical probe (CP) in the source chamber and a planar probe (PP) in the target chamber, were used to diagnose the plasma parameters. The PP was also used to detect the wave signals. In the experimental chamber, a retarding-field-energy-analyzer (RFEA) located 100 mm from the SG2 was used to measure the ion distribution function, from which the Mach number and the density proportion of the ion beam can be inferred. A small negatively biased grid (80 mm in diameter and 65% transparency) was used as the excitation grid (EG) to launch the ion waves, which was located 240 mm away from the SG2.

In the present experiment, the two chamber walls, the anode mesh, and the SG1 were all grounded. The voltage on SG2 was negative and adjustable so that the ion beam energy can be controlled. From the data of the RFEA, it is inferred that the plasma in the experimental chamber consists of two ion groups, one is the background and the other is the beam,[29] so that the ion-beam–plasma system is formed. The beam Mach number changes (not monotonically) with the bias on SG2 (V_{SG2}). The beam Mach number is in the range $\sim$ 5.6–6.6 when V_{SG2} changes from -40 V to -8 V, in which the plasma parameters also vary. Figure 2 shows the variations of the electron density n_e, temperature T_e, and the beam proportion α (the ratio of the beam density to the total ion density) versus the beam Mach number (obtained by varying V_{SG2}). It shows that n_e has a slight increase but T_e and α have a slight decrease when the Mach number increases from 5.6 to 6.6. The typical parameters in the region between the SG2 and EG are $n_e \sim 9.5 \times 10^{13}$ m^{-3}, $T_e \sim 1.2$ eV, $\alpha \sim 0.6$, and the beam Mach number ~ 6 when $V_{SG2} = -26$ V.

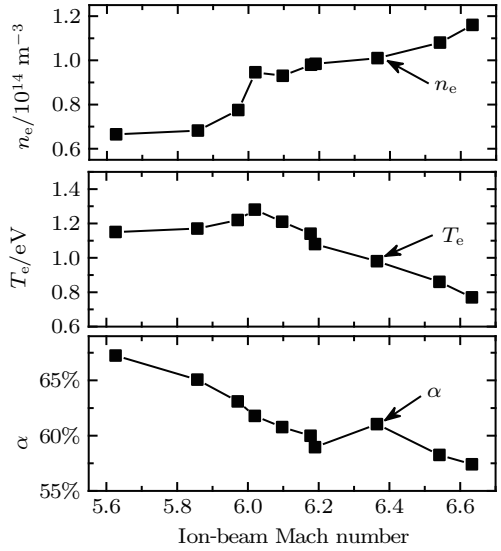


Fig. 2. The electron density n_e, temperature T_e, and the density ratio between the beam and the total ions α, versus the ion-beam Mach number.

3. Characteristics of excited wave signals in the upstream direction

3.1. Wave excitation

In most previous experiments, the ion waves were launched by applying a voltage pulse either between the source and target chambers[6] or to the separation grid[11] in double-plasma devices. Here, we utilized an additional excitation grid (EG) to launch the ion waves, so that the grid used to generate the ion beam and that used to launch the waves were different, which enabled us to launch the waves both in the upstream and downstream directions. The EG was negatively biased at dc voltage -52 V so that a dc ion sheath formed near it. In order to launch the ion density perturbation, a hyperbolic tangent shaped ramp voltage signal, generated by a programmable signal generator, was superimposed to the dc voltage of the EG so that its bias is

$$V_{EG} = -52 + V_{pp} \tanh(t/\tau) \,, \tag{1}$$

where V_{pp} and τ are the adjustable peak-to-peak amplitude and rise time of the ramp voltage.

The ion waves were most efficiently excited when τ was of the order of f_{pi}^{-1}, which was about a few microseconds in this experiment, where f_{pi} is the ion plasma frequency. The

excited wave signals were detected by the moveable PP. The PP was positively biased at 12.4 V to detect the perturbation of the electron density, which is approximately equal to the ion density perturbation since the charge neutrality holds for the low frequency ion waves. The wave signals were recorded by a digital oscilloscope. By moving the PP to different positions and recording the corresponding signals, the wave evolution could be observed and the signal velocity could be obtained using the time-of-flight (TOF) method.

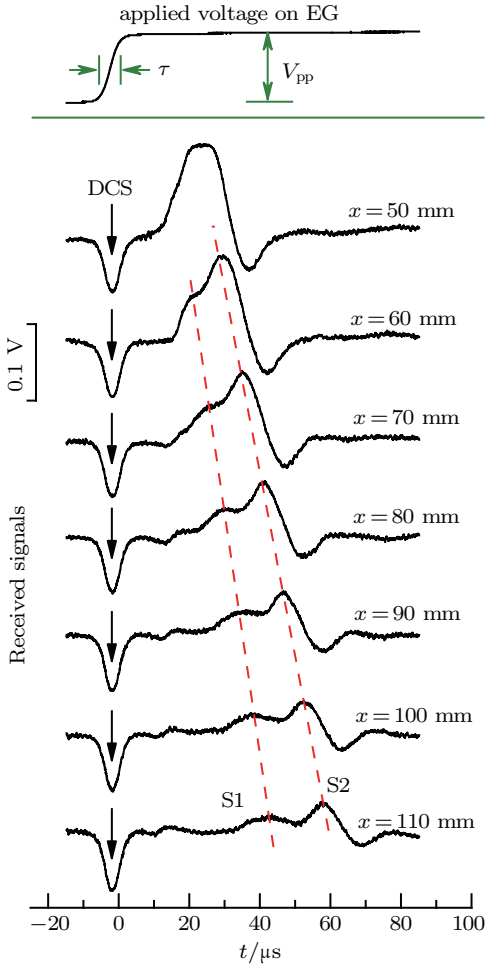


Fig. 3. (color online) Evolution of the received signals, S1 and S2, propagating along the upstream direction, with respect to the distance from the excitation grid that is located at $x = 0$. The parameters are $V_{SG2} = -28$ V, $V_{pp} = 12$ V, and $\tau = 11.1$ μs. The two dashed lines indicate the peak positions of S1 and S2. DCS stands for directly couple signal due to electromagnetic induction.

Figure 3 shows the evolution of the received wave signals at different positions relative to the EG in the case when $\tau = 11.1$ μs and $V_{pp} = 12$ V. It can be seen that at the distances $x \leq 50$ mm ($x = 0$ is the location of the EG), the signals of different nature do not have sufficient time to be distinguished and appear as a flat envelope. At the distance $x = 60$ mm, the signals start to separate. After $x \geq 70$ mm, two separate signals, S1 and S2, with different velocities as shown by the two dashed lines in the figure, emerge clearly and retain their shapes when they propagate away from the EG except the attenuation of their amplitudes. These signals have quite different natures as will be shown below. Note that this observation is opposed to that in the downstream case where four different wave signals were observed.[28]

3.2. Variation of the wave signals with respect to τ

In order to see the difference between the two signals, we investigate their dependence on the excitation parameters. We first keep V_{pp} at 12 V and vary the ramp rise time τ from 9.23 μs to 12.5 μs in the case when $V_{SG2} = -28$ V. Figure 4 shows the evolution of the wave signals, received at $x = 90$ mm, with respect to τ. It can be seen that the first signal S1 moves rightward with the increase of τ but the second signal S2 is almost immobile, indicating that S1 propagates slower when τ increases. The peak value of S1 is nearly unchanged but that of S2 increases. Figure 5 is a plot of the signal velocity, obtained using the TOF method, versus τ. It is shown that the signal velocity of S1 decreases with the increase of τ while that of S2 is independent of τ.

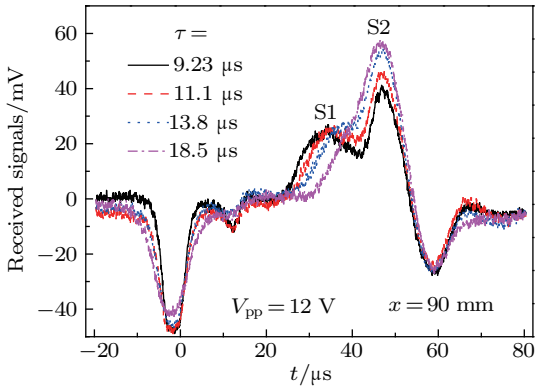


Fig. 4. (color online) Variation of the received signals with respect to τ when $V_{pp} = 12$ V and $V_{SG2} = -28$ V.

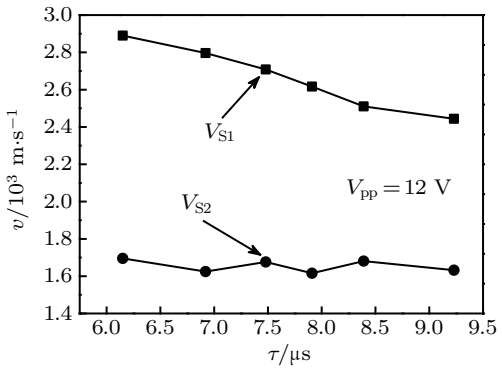


Fig. 5. Velocities of the received signals versus τ when $V_{pp} = 12$ V and $V_{SG2} = -28$ V.

3.3. Variation of the wave signals with respect to V_{pp}

When τ is kept at 11.1 μs, the variation of the wave signals received at $x = 90$ mm with respect to V_{pp} is shown in Fig. 6. With the increase of V_{pp}, the signal S1 moves leftward

while S2 remains almost stationary, indicating that S1 propagates faster in this case. The signal velocity versus V_{pp} is shown in Fig. 7. It shows that the velocity of S1 increases but that of S2 changes little with the increase of V_{pp}. The peak values of both signals increase with V_{pp}, which is obvious since the excitation voltage on EG is increased.

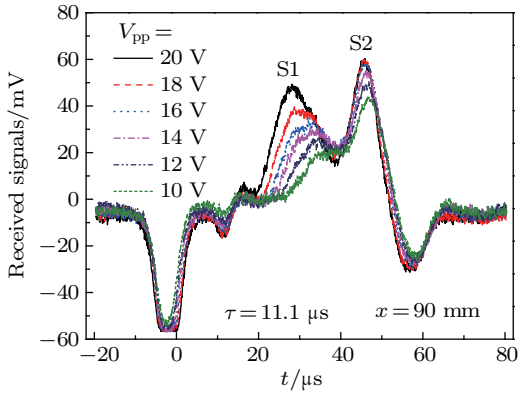


Fig. 6. (color online) Variation of the received signals with respect to V_{pp} when $\tau = 11.1$ μs and $V_{SG2} = -28$ V.

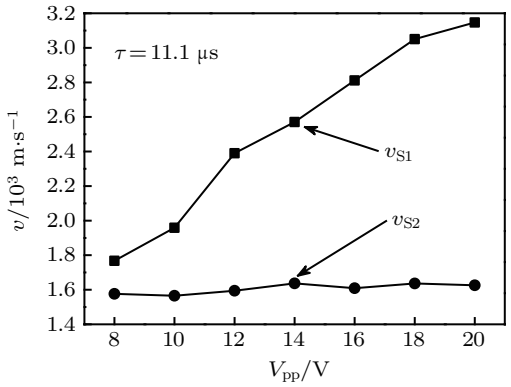


Fig. 7. Velocities of the received signals versus V_{pp} when $\tau = 11.1$ μs and $V_{SG2} = -28$ V.

3.4. Variation of the wave signals with respect to the beam Mach number

When the excitation parameters were fixed at $\tau = 11.1$ μs and $V_{pp} = 12$ V, the Mach number of the ion-beam, M_b, was varied by changing the bias on SG2. The variation of the received wave signals with respect to M_b is shown in Fig. 8. It shows that the peak values of the signals change with M_b. However, the peak positions of the signals change little. Figure 9 shows the dependence of the signal velocities on M_b. The velocity of S1 has a tendency to slightly increase but shows complex variation. The velocity of S2 only shows a tendency of a slight decrease. Thus, the signal velocities only weakly depend on the beam Mach number.

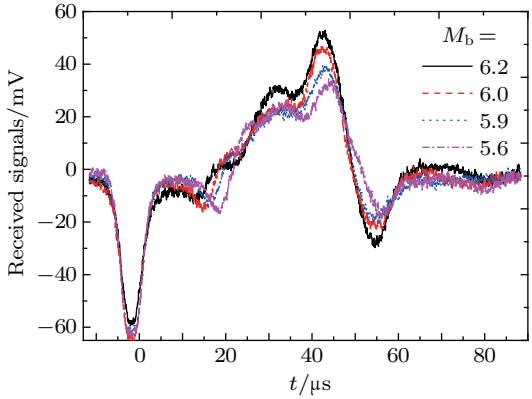


Fig. 8. (color online) Variation of the received signals with respect to the ion-beam Mach number when $\tau = 11.1$ μs and $V_{pp} = 12$ V.

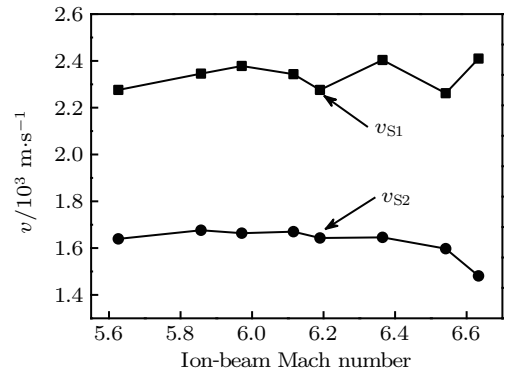


Fig. 9. Velocities of the received signals versus the ion-beam Mach number when $\tau = 11.1$ μs and $V_{pp} = 12$ V.

4. Identification of the burst ions

The burst ions are a group of ions which are generated by the rapidly varying sheath potential near the excitation grid. If the ion sheath near the negatively biased EG is stationary, the ions on one side of the EG will be accelerated toward the EG and then decelerated when leaving the EG on the opposite side, with the exit velocity equal to the incident one. Imagine that if the sheath potentials are instantly raised, the ions in the sheath regions will have a kinetic energy increase because of energy conservation. These ions will burst out at the exit side into the bulk plasma with energy larger than that at the incident side. They will arrive at the probe and form a wave-like signal on the oscilloscope. This burst ion signal is termed as pseudo-wave[24] because it is not a normal mode of the plasma. It depends sensitively on the applied excitation voltage on the EG. The average velocity of the burst ions may be written as[27]

$$v_b \sim c_s \sqrt{M^2 + \frac{2eV_{pp}}{T_e} \frac{1}{f_{pi}\tau}}\,, \tag{2}$$

where M is the ion Mach number in the bulk plasma, $c_s = (T_e/m_i)^{1/2}$ is the ion-acoustic speed, and m_i is the ion mass.

In the upstream direction, the burst ions originate from the background ions in the sheath region of the EG and are accelerated out of the upstream sheath by the applied ramp voltage, which is different from the case in the downstream direction where the burst ions originate from both the background and the beam ions. Since the background ions have zero velocity in the bulk plasma, $M = 0$. Thus, from Eq. (2), v_b increases

with the increase of V_{pp} but decreases with the increase of τ. This property is the same as that of S1 observed in Section 3. Therefore, the signal S1 can be identified as the burst ion signal.

Equation (2) also shows that the burst ion velocity in the upstream direction does not depend on the ion-beam Mach number. However, as shown in Fig. 2, the plasma parameters, i.e., T_e and n_e and thus f_{pi}, are weakly related to the beam Mach number. This may explain the slight variation of the S1 velocity with respect to the beam Mach number as shown in Fig. 9.

5. Identification of the ion-acoustic wave

The characteristics of the normal modes are determined by the dispersion relation. In an idealized cold ion-beam–plasma system, the dispersion equation for the wave number k and frequency ω can be written as

$$1+\frac{1}{k^2\lambda_{De}^2}-\frac{\omega_{pi}^2}{\omega^2}-\frac{\omega_{bi}^2}{(\omega-ku)^2}=0\,, \tag{3}$$

where $\lambda_{De}=(\varepsilon_0 T_e/e^2 n_e)^{1/2}$ is the electron Debye length, $\omega_{bi}=(e^2 n_{bi}/\varepsilon_0 m_i)^{1/2}$ and $\omega_{pi}=(e^2 n_{pi}/\varepsilon_0 m_i)^{1/2}$ are the plasma frequencies of the beam and background ions, n_{bi} and n_{pi} are the beam and background ion densities, respectively, u is the velocity of the ion beam, and ε_0 is the vacuum dielectric constant.

Solving Eq. (3) is equivalent to finding the solution of the following algebraic equation:

$$F(\omega,u)=\frac{(1-\alpha)k^2c_s^2}{\omega^2}+\frac{\alpha k^2 c_s^2}{(\omega-ku)^2}=1+k^2\lambda_{De}^2\,, \tag{4}$$

where $\alpha=n_{bi}/n_e$ and the quasi-neutrality condition $n_e=n_{pi}+n_{bi}$ has been used. For given k and u, ω can be obtained graphically by the intersections of the function $F(\omega,u)$ with the straight line $F=1+k^2\lambda_{De}^2$, as depicted in Fig. 10. It is obvious that in the downstream direction, there are three solutions, i.e., three normal modes. However, in the upstream direction, there is only one solution, which is the background ion-acoustic wave. Under the quasi-neutrality approximation, $k\lambda_{De}\ll 1$, and in the case $\omega\ll ku$, the backward propagating ion-acoustic wave has the phase velocity

$$v_\phi=\omega/k\approx(1-\alpha)^{1/2}c_s\,, \tag{5}$$

which is independent of the characteristics of the excitation voltage as well as the ion beam velocity. The observed characteristics of the signal S2 in Section 3 are coincident with that of Eq. (5). Thus, the signal S2 can be identified as the ion-acoustic wave propagating in the direction upstream to the ion beam.

Equation (5) shows that the phase velocity of the ion-acoustic wave does not explicitly depend on the beam Mach number. The weak dependence of the S2 velocity on the beam Mach number observed in Fig. 9 is due to the slight variation of α and T_e as shown in Fig. 2.

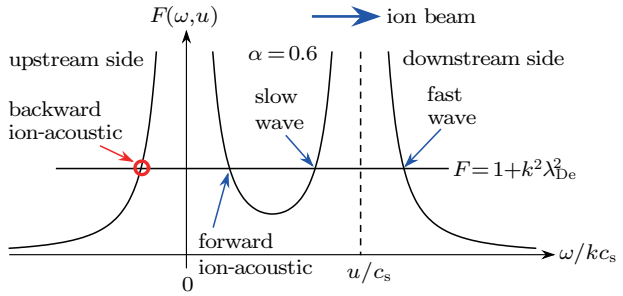


Fig. 10. (color online) Possible solutions to the dispersion equation (3). Three waves propagate in the downstream direction and only one wave propagates in the upstream direction.

6. Wave–particle interaction

In Sections 4 and 5, we have identified that S1 is the particle signal of the burst ions whose velocity depends on the excitation characteristics and S2 is the ion-acoustic signal whose velocity is independent of the excitation characteristics. Thus, it is possible to investigate the wave–particle interaction process via observing the evolution of the signals by adjusting the signal velocity of S1. Figure 11 is a plot of the evolution of the received signals. In small τ cases, the velocity of S1 is larger than that of S2. As τ increases, the velocity of S1 decreases gradually. In this process, when the velocity of S1 is approaching to that of S2 (i.e., when signal S1 moves rightwards toward S2 and begins to overlap with S2), the effect of inverse Landau damping should occur, leading to the enhancement of the signal S2. Figure 12 shows the variation of the peak value of S2 with respect to τ. It shows that the peak value increases as τ increases, reaches a maximum value at which the velocity of S1 is close to that of S2, and then decreases again when S1 immerges into S2. For larger values of τ, the burst ions are not efficiently produced. Thus, it is unable to observe the S1 signal lagging behind S2.

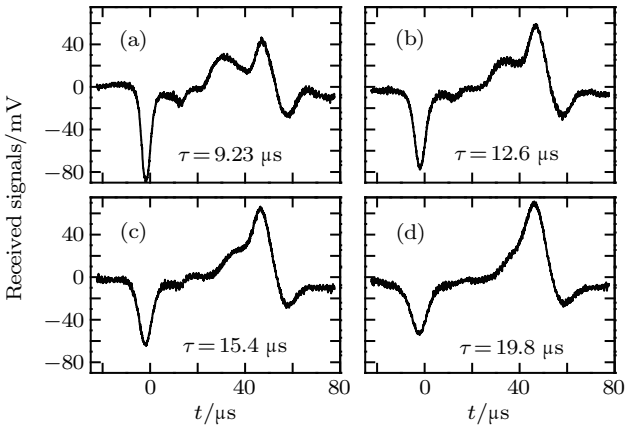


Fig. 11. The evolution of the signals received at $x=90$ mm with respect to τ in the case $V_{pp}=14$ V.

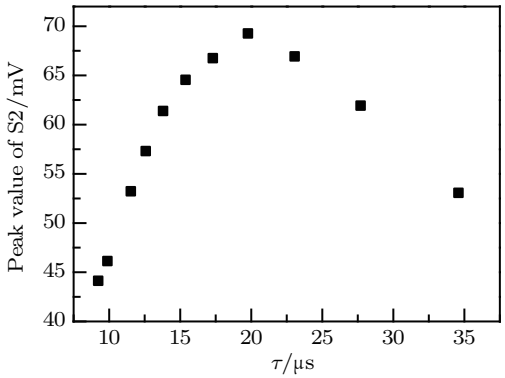


Fig. 12. The peak value of the ion acoustic signal versus τ at $x = 90$ mm in the case $V_{pp} = 14$ V.

7. Conclusion

Two ion wave signals propagating along the upstream direction in the ion-beam–plasma system were excited and studied in the double-plasma device. From the dependence of the signal velocities on the excitation characteristics, it was identified that one signal is the particle signal composed of burst ions and the other signal is the plasma normal mode of the background ion-acoustic wave. The signal velocity of the burst ions decreases with the increase of the rise time and with the decrease of the peak-to-peak amplitude of the ramp voltage applied to the excitation grid used to launch the waves. In the upstream direction, there was only one normal mode observed, which is consistent with the theoretical prediction, as opposed to the case in the downstream direction in which there were three normal modes observed.

By gradually increasing the ramp rise time, it was observed that the burst ion velocity decreases from larger than to approaching the ion-acoustic velocity. Thus, the wave–particle interaction process between the ion-acoustic signal and the burst ion signal was observed, which led to the enhancement of the ion-acoustic wave signal.

References

[1] Hershkowitz N, Romesser T, Knorr G and Goertz C K 1974 *Phys. Rev. Lett.* **33** 754
[2] Gréesillon D and Doveil F 1975 *Phys. Rev. Lett.* **34** 77
[3] Sato N, Sugai H and Hatakeyama R 1975 *Phys. Rev. Lett.* **34** 931
[4] Fujita T, Ohnuma T and Adachi S 1975 *Phys. Fluids* **18** 1216
[5] Brakenhoff G J, Baan A and Matitti T 1973 *Plasma Phys.* **15** 157
[6] Honzawa T 1984 *Phys. Rev. Lett.* **53** 1915
[7] Bonhomme G, Pierre T, Leclert G and Trulsen J 1991 *Plasma Phys. Control. Fusion* **33** 507
[8] Lee S G, Diebold D A, Hershkowitz N and Moroz P 1996 *Phys. Rev. Lett.* **77** 1290
[9] Nagasawa T and Honzawa T 1996 *Phys. Plasmas* **3** 2864
[10] Nakamura Y and Komatsuda K 1998 *J. Plasma Phys.* **60** 69
[11] Franck C, Klinger T and Piel A 1999 *Phys. Lett. A* **259** 152
[12] Nakamura Y, Bailung H and Ichiki R 2004 *Phys. Plasmas* **11** 3795
[13] Rapson C, Grulke O, Matyash K and Klinger T 2014 *Phys. Plasmas* **21** 052103
[14] Tokluoglu E and Kaganovich I D 2015 *Phys. Plasmas* **22** 040701
[15] Lotov K V, Timofeev I V, Mesyats E A, Snytnikov A V and Vshivkov V A 2015 *Phys. Plasmas* **22** 024502
[16] Koshkarov O, Smolyakov A I, Kaganovich I D and Ilgisonis V I 2015 *Phys. Plasmas* **22** 052113
[17] Deka M K, Adhikary N C, Misra A P, Bailung H and Nakamura Y 2012 *Phys. Plasmas* **19** 103704
[18] Sharma S K and Bailung H 2010 *Phys. Plasmas* **17** 032301
[19] Wong A Y, Motley R W and D'Angelo N 1964 *Phys. Rev.* **133** A436
[20] Ma J X, Li Y F, Xiao D L, Li J J and Li Y R 2005 *Rev. Sci. Instrum.* **76** 062205
[21] Lonngren K E, Khazei M, Gabl E F and Bulson J M 1982 *Plasma Phys.* **24** 1483
[22] Gabl E F and Lonngren K E 1984 *Plasma Phys. Control. Fusion* **26** 799
[23] Raychaudhuri S, Gabl E F, Tsikis E K and Lonngren K E 1984 *Plasma Phys. Control. Fusion* **26** 1451
[24] Alexeff I, Jones W D and Lonngren K 1968 *Phys. Rev. Lett.* **21** 878
[25] Yi S, Bai E W and Lonngren K E 1997 *Phys. Plasmas* **4** 2436
[26] Honzawa T and Nagasawa T 1997 *Phys. Plasmas* **4** 3954
[27] Xiao D L, Ma J X, Li Y R, Li Y F and Yu M Y 2007 *Phys. Plasmas* **14** 092104
[28] Wu F, Ma J X, Wei Z A, Yi K Y and Wang T T 2016 *Phys. Plasmas* **23** 102118
[29] Wei Z A, Ma J X, Li Y R, Sun Y and Jiang Z Q 2016 *Plasma Sci. Technol.* **18** 1076